International Journal of Heat and Technology
Vol. 37, No. 3, September, 2019, pp. 779-786
Journal homepage: http://iieta.org/journals/ijht

Numerical Study of Natural Convection Between Two Coaxial Inclined Cylinders

Sihem Gourari[1], Fateh Mebarek-Oudina[2], Ahmed Kadhim Hussein[3], Lioua Kolsi[4,5*], Walid Hassen[5], Obai Younis[6,7]

[1] Department of Mechanical Engineering, Faculty of Technology, University of 20 Août 1955 – Skikda, Skikda, Algeria
[2] Department of Physics, Faculty of Sciences, University 20 août 1955 – Skikda, B.P 26 Route El-Hadaiek, Skikda 21000, Algeria
[3] Mechanical Engineering Department, College of Engineering, University of Babylon, Babylon City 51002, Hilla, Iraq
[4] Mechanical Engineering Department, College of Engineering, Hail University, 2240, Hail City, Saudi Arabia
[5] Laboratoire de Métrologie et des Systèmes Énergétiques, École Nationale d'Ingénieurs, University of Monastir, 5000, Monastir, Tunisia
[6] Department of Mechanical Engineering, College of Engineering at Wadi Addwaser, Prince Sattam Bin Abdulaziz University, 18311, KSA
[7] Department of Mechanical Engineering, Faculty of Engineering, University of Khartoum, 11115, Sudan

Corresponding Author Email: lioua_enim@yahoo.fr

https://doi.org/10.18280/ijht.370314

Received: 4 June 2018
Accepted: 23 July 2019

Keywords:
numerical simulation, finite volume method, natural convection, coaxial cylinders, heat source

ABSTRACT

The natural convection flow of water between two coaxial cylinders where the inner cylinder generates a constant heat source is numerically studied. The outer cylinder is cold while the top and bottom walls are thermally insulated. For a laminar flow and an inclination angle equal 0°, 45°, 90° the results are determined in the form of contours of the isotherms and streamlines, average Nusselt number in the annular space. The results show that the average Nusselt number is growing with increasing Rayleigh numbers. The best heat transfer is obtained for the inclination angle 90°.

1. INTRODUCTION

Among the best renewable energy sources with minimal environmental impact is solar energy. In recent years, natural convection problems have attracted more attention because of its large applications, such as solar energy systems in energy sensing systems, which help to better understand this thermal phenomenon in cavities inclined. Natural convection is a fundamental phenomenon in many types of collectors and receivers. The difference in temperature causes a natural convection and the heat loss is achieved solely by conduction. It is well known that natural convection phenomena are quite sensitive to boundary conditions. From where we can find a very large number of studies in the literature concerning this phenomenon [1-6]. In solar collectors, the insulating air is generally confined in an enclosure formed by the sides of the collector, one or two of the panes, or the absorbing plate. If convection suppression walls (or honeycomb structures) are used in the collector, convection occurs in the volume enclosed by these partitions and by the windows or the absorber. Some cavity elements in the concentration collectors have open solar radiation that improves the opening, and because of this opening on one or more walls, the natural convection circuit is incomplete [7].

Our knowledge of convective heat transfer in ducts is widely developed and, when properly applied, this available information can be directly used in thermal analysis and solar collector design.

Generally, the flow rate is very low in the liquid-heating collector ducts, and is therefore laminar and may develop for a good fraction along the tube. So we will have to examine them starting with the application of classical criteria.

Noting that most of these criteria have been established for constant temperature or heat flux conditions, irrespective of buoyancy effects, i.e. for conditions that do not accurately represent the situation of the sensors.

Numerical studies have been conducted to study natural convection inside a solar collector. The working fluid inside the solar collector is another challenge for the researchers in the field. Rehena et al. [8] presented a numerical investigation of the influence of physical parameters, wave amplitude, and wave number on the natural convection flow of the boundary layer inside a solar collector with water-Al_2O_3 nanofluid. Rahman et al. [9] studied the double-diffusive natural convection in a triangular solar collector where the effects of Rayleigh number and buoyancy rate are presented with streamlines, isotherms and iso-concentrations as well as heat and mass transfer rates. Other interesting works related to the subject can be found [10-18].

The effect of the inclination angle on the natural convection of a flow between two coaxial cylinders whose internal cylinder generates a constant heat source has never been the subject of a previous study. Our objective is to determine the thermal and dynamic field that arise on this type of flow as well the effect of Ra and the inclination angle on the heat transfer.

2. GEOMETRY & MATHEMATICAL MODEL

Pure water with a Prandt number, Pr=6.3 is the fluid chosen in this modest study. This fluid is located in the space between two coaxial cylinders where the inner cylinder generates a constant heat source, the outer cylinder is cold while the lower

and upper walls are adiabatic. γ is the inclination angle of the annulus (Figure 1).

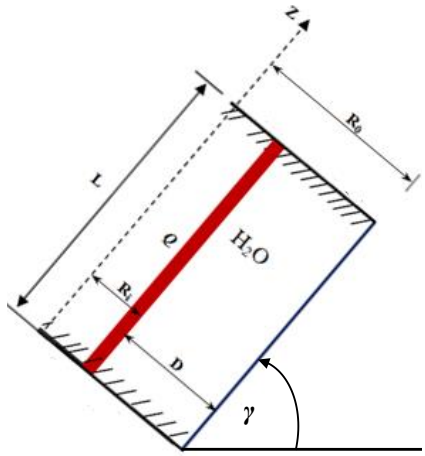

Figure 1. Geometry of studied configuration

The space between the two cylinders, $(R_o - R_i)$, is used as a characteristic length, the thermal diffusion time through space, $(R_o - R_i)^2/\alpha$, is the scalar time, and the scalar temperature is $Q(R_o - R_i)/\kappa$, where κ is the thermal conductivity and α is the thermal diffusivity of the fluid. The dimensionless temperature relative to the temperature of the outer cylinder is $\Theta = (T - T_f)\kappa/Q(R_o - R_i)$. [19]

Based on reference [4], the dimensional governing equations are:

$$\frac{\partial(ru)}{\partial r}+\frac{\partial(rv)}{\partial z}=0 \tag{1}$$

$$\rho\left(\frac{\partial u}{\partial \tau}+u\frac{\partial u}{\partial r}+v\frac{\partial u}{\partial z}\right)=-\frac{\partial p}{\partial r} +\mu\left(\frac{1}{r}\frac{\partial}{\partial r}\left(r\frac{\partial u}{\partial r}\right)+\frac{\partial^2 u}{\partial z^2}-\frac{u}{r^2}\right) +(\rho\beta)\,g\,(T-T_C)\sin(\gamma) \tag{2}$$

$$\rho\left(\frac{\partial v}{\partial \tau}+u\frac{\partial v}{\partial r}+v\frac{\partial v}{\partial z}\right)=-\frac{\partial p}{\partial z} +\mu\left(\frac{1}{r}\frac{\partial}{\partial r}\left(r\frac{\partial v}{\partial r}\right)+\frac{\partial^2 v}{\partial z^2}\right) +(\rho\beta)\,g\,(T-T_C)\cos(\gamma) \tag{3}$$

$$\frac{\partial T}{\partial \tau}+u\frac{\partial T}{\partial r}+v\frac{\partial T}{\partial z}=\alpha\left(\frac{1}{r}\frac{\partial}{\partial r}\left(r\frac{\partial T}{\partial r}\right)+\left(\frac{\partial^2 T}{\partial z^2}\right)\right) \tag{4}$$

The flow is governed by the Rayleigh number, $Ra=\frac{g\beta QD^4}{k\upsilon\alpha}$, and the number, $\Pr=\frac{\upsilon}{\alpha}$, thus these geometrical parameters: the aspect ratio $A_r=\frac{L}{D}$, radii ratio, $\lambda=\frac{R_0}{R_i}$.

where, $\alpha=\kappa/\rho C_p$ is the thermal diffusivity of the liquid, k is the thermal conductivity and C_p its specific heat at a constant pressure.

Based on the work of Mebarek-Oudina [19], the governing dimensionless equations are:

$$\frac{\partial(RU)}{\partial R}+\frac{\partial(RV)}{\partial Z}=0 \tag{5}$$

$$\frac{\partial U}{\partial t}+u\frac{\partial U}{\partial R}+V\frac{\partial U}{\partial Z}=-\frac{\partial P}{\partial R} +\left(\frac{1}{R}\frac{\partial}{\partial R}\left(R\frac{\partial U}{\partial R}\right)+\frac{\partial^2 U}{\partial Z^2}-\frac{U}{R^2}\right) +\frac{1}{\Pr}\cdot Ra\cdot\Theta\sin(\gamma) \tag{6}$$

$$\frac{\partial V}{\partial t}+U\frac{\partial V}{\partial R}+V\frac{\partial V}{\partial Z}-\frac{Ra}{\Pr}\cdot\Theta=-\frac{\partial P}{\partial Z} +\left(\frac{1}{R}\frac{\partial}{\partial R}\left(R\frac{\partial V}{\partial R}\right)+\frac{\partial^2 V}{\partial Z^2}\right) +\frac{1}{\Pr}\cdot Ra\cdot\Theta\cos(\gamma) \tag{7}$$

$$\frac{\partial\Theta}{\partial t}+U\frac{\partial\Theta}{\partial R}+V\frac{\partial\Theta}{\partial Z}=\frac{1}{\Pr}\left(\frac{1}{R}\frac{\partial}{\partial R}\left(R\frac{\partial\Theta}{\partial R}\right) +\left(\frac{\partial^2\Theta}{\partial Z^2}\right)\right) \tag{8}$$

The initial and boundary conditions in dimensionless form are:

$$\text{For } t=0,\ U=V=\Theta=0 \tag{9}$$

For $t>0$

$$\text{at R = 1: } U=V=0,\ \frac{\partial\Theta}{\partial R}=-1 \tag{10a}$$

$$\text{at R = 2: } U=V=0,\ \Theta=0 \tag{10b}$$

$$\text{at Z = 0: } U=V=0,\ \frac{\partial\Theta}{\partial z}=0 \tag{10c}$$

$$\text{at Z}=\frac{L}{D}\text{: } U=V=0,\ \frac{\partial\Theta}{\partial Z}=0 \tag{10d}$$

3. NUMERICAL SOLUTION

The results of this study are obtained using the reference calculation code of Mebarek-Oudina [19]. This house code validated by the author with the results of Sankar et al. [20] has been adopted for the resolution of the studied

configuration.

3.1 Grid independency test

The area of large velocity and temperature gradients requires a larger number of nodes to resolve specific flow characteristics, and reduce numerical errors. So several non-uniform grids will be used in this area (near the annulus walls). In order to examine the effect of the mesh on the numerical solution, a number of sizes are used to study the independence of the grid: 52×104, 72×144, 92×164 et 100× 200 nodes.

By examining the curves shown in (Figure 2), we observe a variation less than 1 % of the values calculated between 100 × 200 and 92 × 164 or 92 × 164 and 72 × 144. For this, the grid corresponding to 92 × 164 nodes are adopted for all numerical simulations, in order to optimize the CPU time and the cost of the calculations.

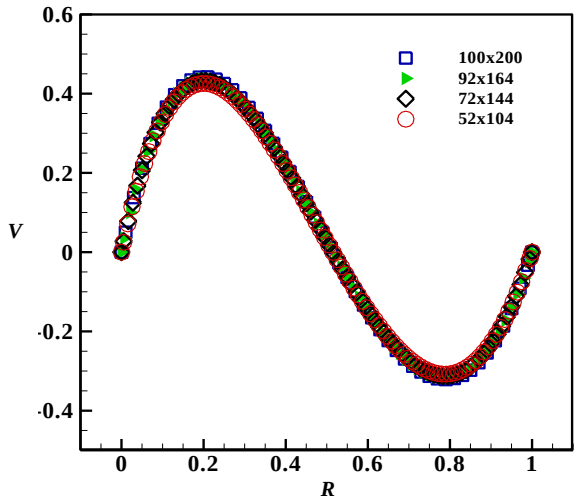

Figure 2. Radial distribution of dimensionless axial velocity for various grids (52×104, 72×144, 92×164, 100×200), A_r=2 and Rayleigh number, Ra=75

4. RESULTS AND DISCUSSION

In this paper the natural convection between two coaxial cylinders has been studied numerically with a focus on the effect inclination angle on heat.

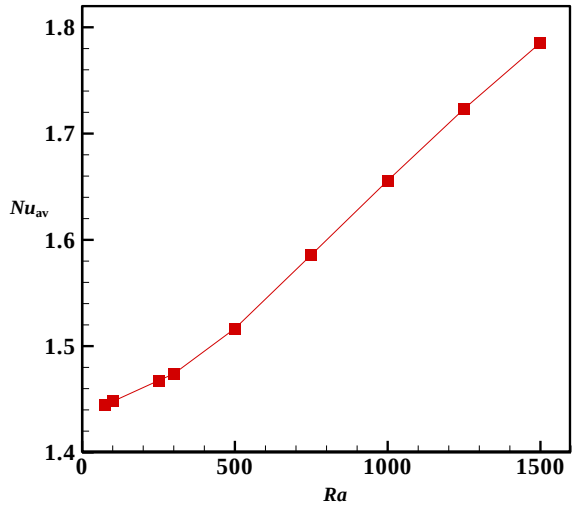

Figure 3. Variation of the average Nusselt number versus Rayleigh number, γ=90°, λ=2 and A_r=2

Figure 3 presents the effect of Rayleigh number on average Nusselt number. As an obvious result the heat transfer increases with increasing Ra.

Figure 4 presents the temperature field and the flow structure for different Ra, γ=90° and A_r=2.

For low Ra numbers, the isothermal lines are almost parallel to the vertical walls without any deformation, which indicates that the conductive transfer mode reigns. The deformation of it is isothermal appears clearly with the increase in the Ra number indicating the presence of the convective transfer mode.

On Figure 5, distributions of dimensionless temperature along the space between the two cylinders are presented. The distributions are similar for the different chosen values of Rayleigh number. The minimum temperature is detected at the bottom of the cylinders while the maximum value of the temperature is obtained at the top of the cylinders for the high value of Ra in this illustration Ra=1250. The minimum and maximum values of the temperature increase with the growth of the Rayleigh number.

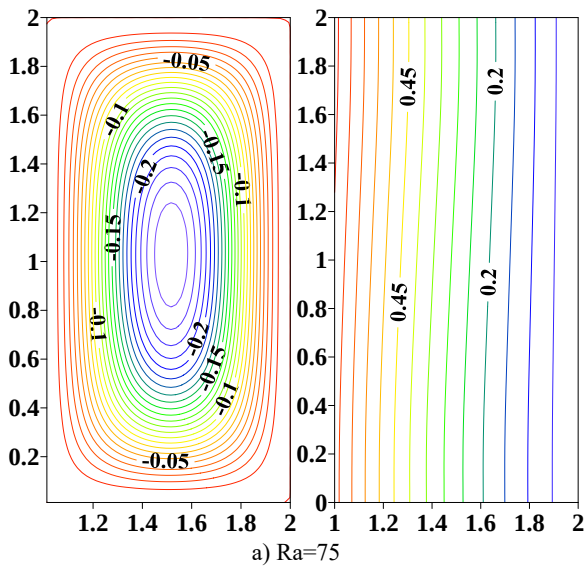

a) Ra=75

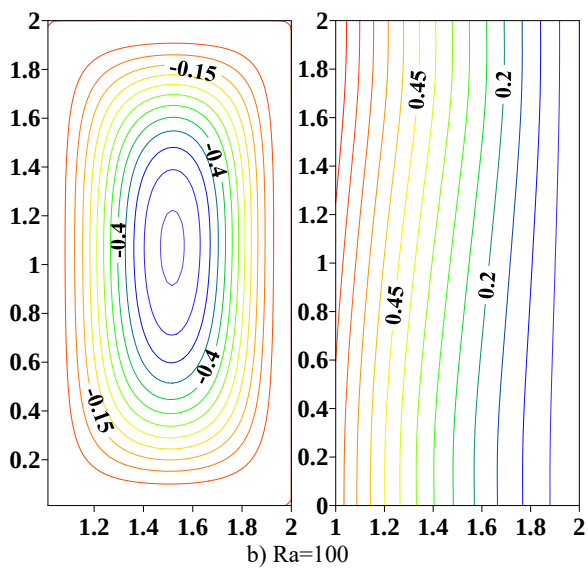

b) Ra=100

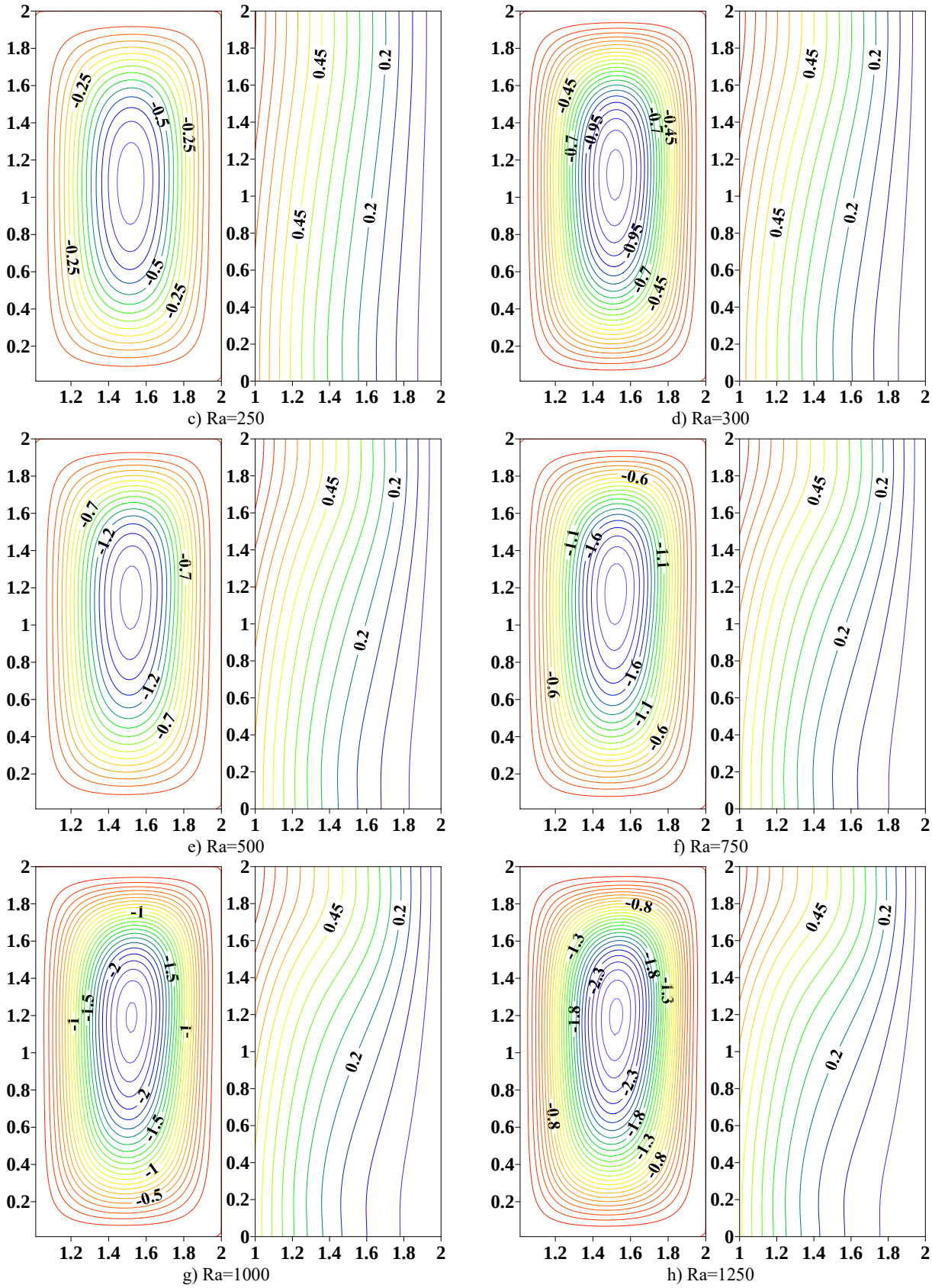

Figure 4. Isotherms (left) and Streamlines (right) for different value of Rayleigh number, γ=90° and A_r=2

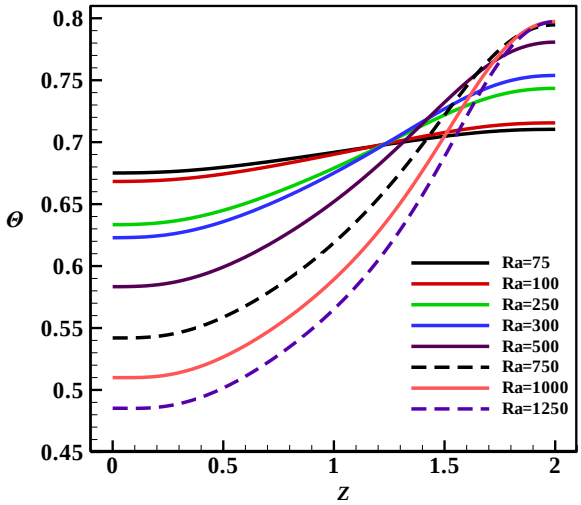

Figure 5. Axial distribution of dimensionless temperature for various Rayleigh numbers, $\lambda=2$ and $A_r=2$

As presented on Figure 6, the minimum and maximum value of the radial velocity increases with increasing Rayleigh number. For all studied case, the maximum value obtained in the first quarter of the radial evolution of the dimensionless velocity (R=0.2), while the minimum value is obtained in the third quarter of its radial evolution (R=0.8).

Figure 7 presents the variation of average Nusselt number versus the inclination angle. The maximal heat transfer is obtained at an inclination angle of 90°. Thus inclination angle can be considered as an important parameter for heat transfer optimization.

Figure 8 illustrates the flow structure and temperature field via the stream function and isotherms respectively. For γ=90° the cavity is vertical and differentially heated. The isotherms are quasi-parallel and the flow is mono-cellular showing that the heat transfer regime is purely conductive due to the relatively low Rayleigh number value (Ra=75). For γ=90° and γ = 45° the configuration is similar to the Rayleigh Bénard case. Isotherms become distorted and flow structure becomes bi-cellular composed by tow counter-rotary cells having different sizes.

Figure 9 presents the radial evolution of the dimensionless axial velocity for three different inclination angles 0°, 45°, 90°. For these three cases studied, the axial velocity takes the same pace. The maximum and minimum values of axial velocity are determined for an inclination of 45°. For the inclination angle 90° the curve of the axial distribution of the temperature is located above that of inclination of 45° with a great distance. While the curve of the temperature distribution for an inclination of 0° is located below the two curves with a small difference compared to the second curve. Therefore, the maximum dimensionless temperature is obtained for an inclination angle of 90° (Figure 10).

5. CONCLUSION

A numerical investigation of the convective flow of water between two coaxial cylinders is made. The inner cylinder generates a constant heat source while the outer cylinder is cold; the lower and upper walls are adiabatic.

The finite volume method with the SIMPLER and THOMAS algorithms are used to model the nonlinear algebraic equation system and obtain solution.

From this study, the following conclusions are obtained:

- For low Rayleigh numbers the conductive heat transfer is dominant;
- The augmentation of the average Nusselt number with the increase in the Rayleigh number;
- Decrease of the minimum value of the stream function with increasing Rayleigh number;
- The inclination angle of 90° has the best heat transfer with a large value of average Nusselt number;

The inclination angle of coaxial cylinders affects the thermal and dynamic field of flow.

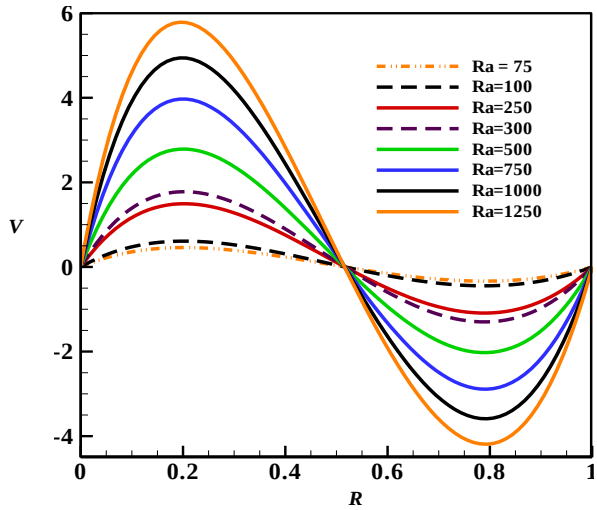

Figure 6. Radial distribution of dimensionless axial velocity for different Rayleigh numbers

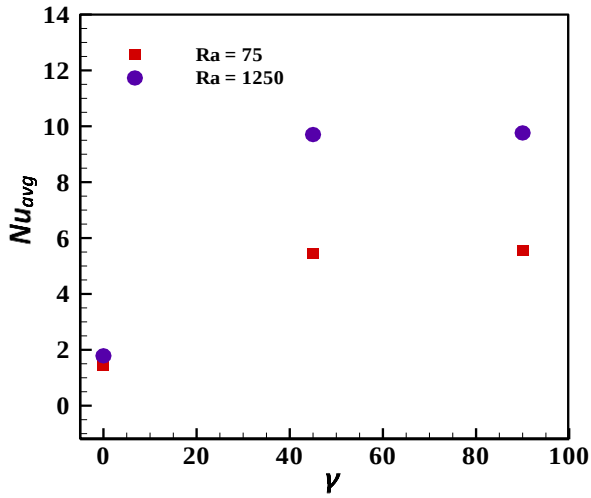

Figure 7. Average Nusselt number for various inclination angles, $\lambda=2$ and $A_r=2$

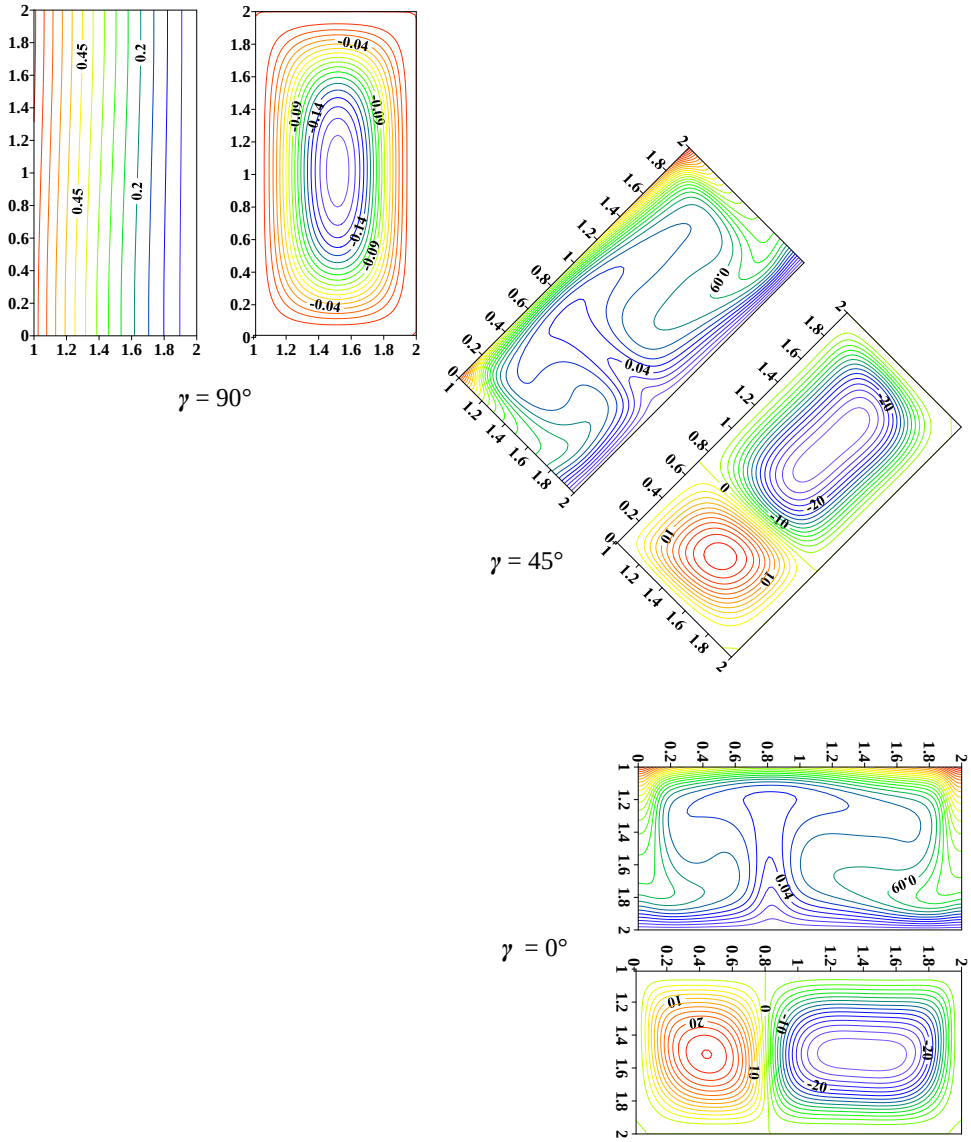

Figure 8. Isotherms (at left) & Streamlines (at right) for various inclination angles and Ra=75

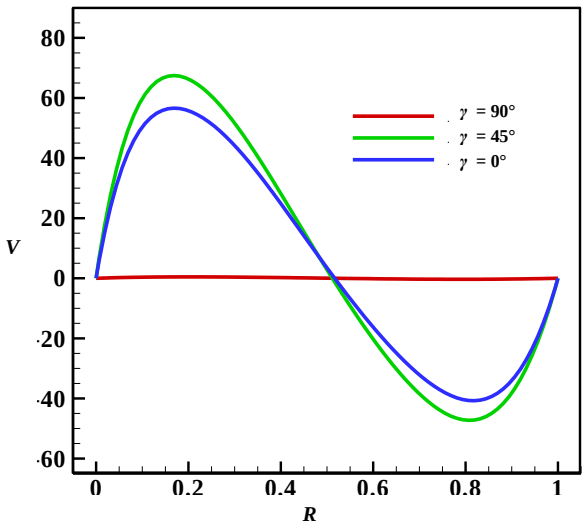

Figure 9. Radial distribution of dimensionless axial velocity for different inclination angles and Rayleigh number, Ra=75

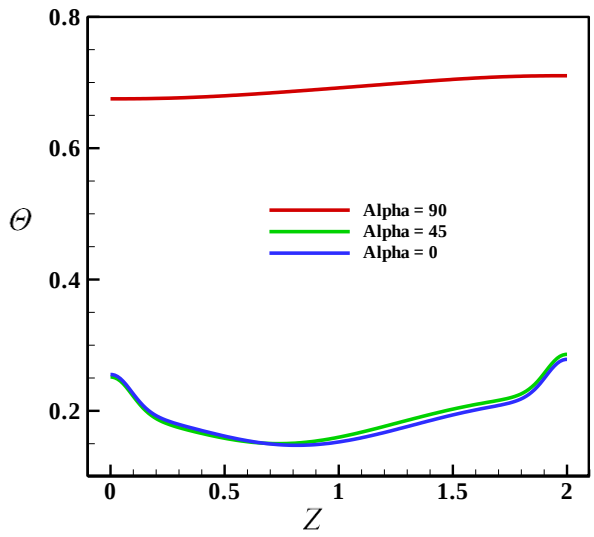

Figure 10. Axial distribution of dimensionless temperature for different inclination angles and a Rayleigh number, Ra=75

REFERENCES

[1] Mebarek-Oudina, F., Bessaïh, R. (2007). Magnetohydrodynamic stability of natural convection flows in Czochralski crystal growth. World Journal of Engineering, 4(4): 15-22.

[2] Mebarek-Oudina, F., Bessaïh, R. (2014). Numerical modeling of MHD stability in a cylindrical configuration. Journal of the Franklin Institute, 351(2): 667-681. https://doi.org/10.1016/j.jfranklin.2012.11.004

[3] Mebarek-Oudina, F., Bessaïh, R. (2016). Oscillatory magnetohydrodynamic natural convection of liquid metal between vertical coaxial cylinders. J. of Applied Fluid Mechanics, 9(4): 1655-1665. https://doi.org/10.18869/acadpub.jafm.68.235.24813

[4] Mebarek-Oudina, F., Bessaïh, R. (2014). Effect of the geometry on the MHD stability of natural convection flows. Institute of Thermomechanics AS CR, v. v. i., Prague, 75: 159-161.

[5] Mebarek-Oudina, F., Bessaïh, R., (2007). Stabilité magnétohydrodynamique des écoulements de convection naturelle dans une configuration cylindrique de type Czochralski. Société Française de Thermique, 1: 451-457.

[6] Mebarek-Oudina, F. (2019). Convective heat transfer of Titania nanofluids of different base fluids in cylindrical annulus with discrete heat source. Heat Transfer - Asian Research, 48: 135-147. https://doi.org/10.1002/htj.21375

[7] De Winter, F. (1990). Solar Collectors, Energy Storage, and Materials. Ed., MIT Press, Cambridge MA.

[8] Rehena, N., Alim, M.A., Chamkha, A.J. (2013). Effects of physical parameters on natural convection in a solar collector filled with nanofluid. Heat Transfer-Asian Research, 42(1): 73-88. https://doi.org/10.1002/htj.21026

[9] Rahman, M.M., Öztop, H.F., Ahsan, A., Kalam, M.A., Varol, Y. (2012). Double-diffusive natural convection in a triangular solar collector. Int Commun Heat Mass Transf., 39(2): 264-269. https://doi.org/10.1016/j.icheatmasstransfer.2011.11.008

[10] Hussain, S., Hussein, A.K. (2010). Numerical investigation of natural convection phenomena in a uniformly heated circular cylinder immersed in square enclosure filled with air at different vertical locations. International Communications in Heat and Mass Transfer, 37(8): 1115-1126. https://doi.org/10.1016/j.icheatmasstransfer.2010.05.016

[11] Hussain, S., Hussein, A.K., Mohammed, R. (2012). Studying the effects of a longitudinal magnetic field and discrete isoflux heat source size on natural convection inside a tilted sinusoidal corrugated enclosure. Computers and Mathematics with Applications, 64: 476-488. https://doi.org/10.1016/j.camwa.2011.12.022

[12] Al-Rashed, A., Kolsi, L., Hussein, A.K., Hassen, W., Aichouni M., Borjini, M. (2017). Numerical study of three-dimensional natural convection and entropy generation in a cubical cavity with partially active vertical walls. Case Studies in Thermal Engineering, 10: 100-110. https://doi.org/10.1016/j.csite.2017.05.003

[13] Al-Rashed, A.A.A.A., Aich, W., Kolsi, L., Mahian, O., Hussein, A.K., Borjini, M.N. (2017). Effects of movable-baffle on heat transfer and entropy generation in a cavity saturated by CNT suspensions: Three-dimensional modelling. Entropy, 19(5): 200. https://doi.org/10.3390/e19050200

[14] Kolsi, L., Abidi, A., Borjini, N.M., Ben Aïssia, H. (2010). The effect of an external magnetic field on the entropy generation in three-dimensional natural convection. Thermal Science, 14(2): 341-352. https://doi.org/10.2298/TSCI1002341

[15] Kolsi, L., Mahian, O., Öztop, H.F., Aich, W., Borjini, M.N., Abu-Hamdeh, N. (2016). 3D buoyancy-induced flow and entropy generation of nanofluid-filled open cavities having adiabatic diamond shaped obstacles. Entropy, 18(6): 232. https://doi.org/10.3390/e18060232

[16] Rahimi, A., Kasaeipoor, A., Malekshah, E.H., Kolsi, L. (2017). Experimental and numerical study on heat transfer performance of three-dimensional natural convection in an enclosure filled with DWCNTs-water nanofluid. Powder Technology, 322: 340-352. https://doi.org/10.1016/j.powtec.2017.09.008

[17] Kasaeipoor, A., Malekshah, E.H., Kolsi, L. (2017). Free convection heat transfer and entropy generation analysis of MWCNT-MgO (15 % − 85 %)/Water nanofluid using Lattice Boltzmann method in cavity with refrigerant solid body-Experimental thermo-physical properties. Powder Technology, 322: 9-23. https://doi.org/10.1016/j.powtec.2017.08.061

[18] Mebarek-Oudina, F., Makinde, O.D. (2018). Numerical simulation of oscillatory MHD natural convection in cylindrical annulus: Prandtl number effect. Defect and Diffusion Forum, 387: 417-427. http://dx.doi.org/10.4028/www.scientific.net/DDF.387.417

[19] Mebarek-Oudina, F. (2017). Numerical modeling of the hydrodynamic stability in vertical annulus with heat source of different lengths. Engineering Science and Technology, 20(4): 1324-1333. https://doi.org/10.1016/j.jestch.2017.08.003

[20] Sankar, M., Hong, S., Do, Y., Jang, B. (2012). Numerical simulation of natural convection in a vertical annulus with a localized heat source. Meccanica, 47(8): 1869-1885. https://doi.org/10.1007/s11012-012-9560-3

NOMENCLATURE

A_r	aspect ratio= L/D [-]
D	length [m]
g	gravitationnel acceleration, m/s^2
L	enclosure height, m
Nu	local Nusselt number [-]
Nu_{av}	average Nusselt number [-]
Pr	Prandtl number [-]
Q	heat flux, W/m^2
Ra	Rayleigh number [-]
R,Z	radial and axial coordinates, respectively
R_i, R_0	inside and outside radii, m
T	temperature, K
t	dimensionless times [-]
Δt	dimensionless times increment [-]
U,V	radial and axial dimensionless velocities, respectively [-]

Greek symbols

α	thermal diffusivity of the fluid, $m^2.s^{-1}$
β	thermal expansion coefficient of the fluid, K^{-1}
γ	inclinaison angle, °
λ	radius ratio [-]
κ	thermal conductivity, m^2/s
ρ	density of the fluid, $kg.m^{-3}$
σ	electrical conductivity, $\Omega^{-1}.m^{-1}$
υ	kinematical viscosity of the fluid, $m^2.s^{-1}$
Θ	dimensionless temperature [-]
Θ_{max}	maximal dimensionless temperature of the hot cylinder [-]
ψ	Dimensionless stream function [-]

Subscripts

c	conditions of cold cylinder
R, Z	radial and axial directions, respectively